

# BViz Photometry of the RR Lyrae Star RU Ceti

Jadon Fickle

Michael L. Allen (ORCID 0000-0002-6047-3315)

Department of Physics and Astronomy, Washington State University, Pullman, WA 99164-2814;

jadon.fickle@wsu.edu; mlfa@wsu.edu

Received September 1, 2021; revised April 14, 2022; accepted April 19, 2022

**Abstract** The RR Lyrae star RU Ceti was observed between October 26 and November 23, 2020. The observations were taken in the B, V, ip, and zs filters, with the telescope images being analyzed using various aperture photometry methods. The period of variation for RU Ceti was found to be  $0.585 \pm 0.020$  day. Theoretical period-luminosity-metallicity relations in the V, ip, and zs filters were used to compute the distance. These distances were  $1641 \pm 77$  parsecs in the V filter,  $1621 \pm 58$  parsecs in the ip filter, and  $1645 \pm 48$  parsecs in the zs filter, for a weighted average of  $1636 \pm 33$  parsecs. The Gaia EDR3 value is  $1699 +83 / -75$  parsecs. The photometric distances are consistent with the parallax determination despite peculiar variations in RU Ceti's light curve.

## 1. Introduction

This research was undertaken as part of OurSolarSiblings' (OSS) education effort to make observational astronomical research more straightforward for students and teachers via a collaboration led by Michael Fitzgerald (Fitzgerald 2018). One goal of this ongoing effort was to use observations to test the theoretical RR Lyrae period-luminosity (PL) relationship in the infrared ip and zs filters given by Cáceres and Catelan (2008) and in the Johnson V filter given by Cáceres and Catelan (2008). We compare against parallax measurements.

RR Lyrae stars are fundamental mode pulsating stars that belong to the horizontal branch. They are often used as standard candles to determine distances within the Milky Way, due to the period-luminosity relations. Empirically derived PL, and period-luminosity-metallicity (PLZ), relations exist for many colors, e.g., Neeley *et al.* (2019), and Cusano *et al.* (2021). These relations exhibit some scatter, thus limiting their precision when used as standard candles, especially for field stars. The RR Lyrae-type star covered in this paper is RU Ceti.

RU Ceti (Figure 1) is classified as an RRab type variable star in the AAVSO Variable Star Index (Watson *et al.* 2006). This can be seen in the nature of the light curve itself, presented in section 3, as RRab light curves are consistently defined by a quick rise to maximum light followed by a gradual decline.

One of the earlier reports of a potential Blazhko effect comes from Kovacs (2005). RU Ceti was reported as a RRab star with “weak” Blazhko effects. Kolenberg *et al.* performed work to determine the Blazhko period of RU Ceti (Kolenberg *et al.* 2008). Both of these papers made use of the All Sky Automated Survey (ASAS) database in order to have data over a long enough range of time to test for the presence of a Blazhko effect and thus a Blazhko period. In the present study, data were not taken over a wide enough range of time to consider the Blazhko nature of this star.

We will cover how we set up our observations of RU Ceti, and discuss what happened to the observations before we received them (section 2) via the data pipelines set up by Las Cumbres Observatory (LCO) and OurSolarSiblings (OSS). Then, we will discuss how we analyzed the observations to

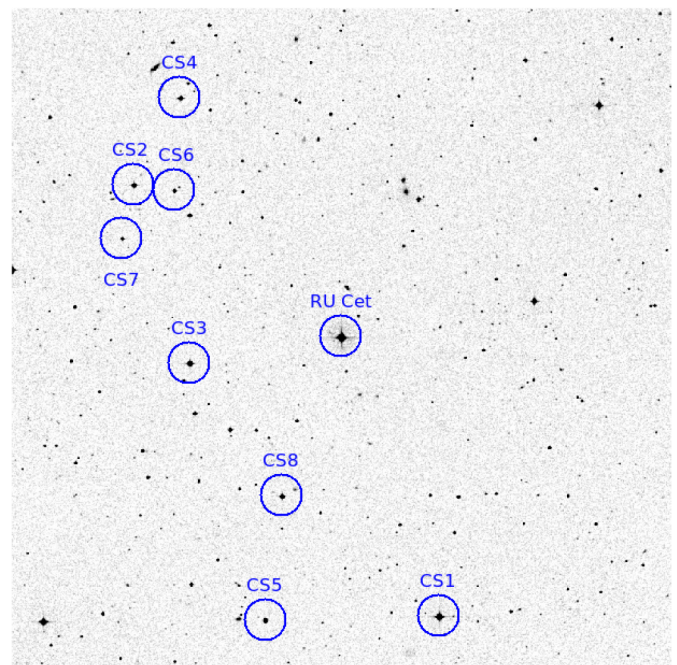


Figure 1. Inverted starfield of observation for RU Ceti. Eight comparison stars were used in the data analysis. The image is  $25 \times 25$  arcminutes. North is up and east is to the left. Image is from the DSS and processed using SAOImageDS9.

Table 1. Basic properties of RU Ceti.

Property	Value	Reference
R.A. (J2000)	$15.16803563^\circ$	Bailer-Jones <i>et al.</i> (2021) (Gaia EDR3)
Dec. (J2000)	$-15.95777516^\circ$	Bailer-Jones <i>et al.</i> (2021)
Sp type	kA3p	Graham and Slettebak (1973)
Variable type	RRab	Watson <i>et al.</i> (2006) (VSX)
Distance	$1699 + 83 / -75$ parsecs	Bailer-Jones <i>et al.</i> (2021)
[Fe/H]	-1.33	Kovacs (2005)
	-1.39	Sandage (1993)
	-1.51	Preston <i>et al.</i> (1991)
	-1.6	Chiba and Yoshii (1998)
	-1.6	Layden (1994)
	-1.6	Layden <i>et al.</i> (1996)
	-1.66	Feast <i>et al.</i> (2008)

determine information about RU Cet (section 3), specifically its period and distance from Earth.

## 2. Observations

RU Cet was observed between October 26 and November 23, 2020. The star was observed in the Johnson-Cousins B and V (e.g., Bessel 1993), SDSS *ip* (Fukugita *et al.* 1996), and Pan-STARRS *zs* (Tonry *et al.* 2012) filters with the Las Cumbres Observatory network of robotic telescopes. The LCO comprises several 2-meter, 1-meter, and 0.4-meter aperture telescopes. Table 2 lists the location and number of observations captured at each location of RU Cet.

All of the observations of RU Cet were performed using the 0.4-meter series of telescopes. Each was equipped with a SBIG STL-6303 CCD camera of format  $3k \times 2k$  pixels, with a pixel size of 0.571 arcsec and a field of view of  $29.2 \times 19.5$  arcmin. Observation cadence was approximately once every four hours, weather permitting. Accounting for poor weather and observation windows expiring, a total of 79 observations of RU Cet were recovered.

Integration times were chosen to achieve a signal-to-noise (S/N) of about 300 on the target star. This is the equivalent of about 100,000 photons integrated. This photon count is where the CCD camera is responding linearly to photon flux and well below the saturation limit. This can be considered the “sweet spot” of the detector, where the noise in the image is attenuated by the true counts from the source, but the image is

Table 2. Telescope locations and number of observations performed by each telescope.

Telescope Location	LCO Telescope Label	Number of Observations
SAAO, Sutherland, South Africa	kb84	32
CTIO, Region IV, Chile	kb26	12
Haleakala Observatory, Maui, USA	kb82	11
Siding Spring Observatory, NSW, Australia	kb56	7
Siding Spring Observatory, NSW, Australia	kb24	7
CTIO, Region IV, Chile	kb29	6
Haleakala Observatory, Maui, USA	kb27	2
McDonald Observatory, Texas, USA	kb92	1
Teide Observatory, Tenerife, Spain	kb98	1

Note: CTIO—Cerro Tololo Inter-American Observatory; SAAO—South African Astronomical Observatory.

not overexposed. These integration times were computed to be 100 seconds in B, 41 seconds in V, 39 seconds in *ip*, and 144 seconds in *zs*. All images recovered were usable.

The LCO’s BANZAI data pipeline (Brown *et al.* 2013) took the raw images from the telescope and corrected them using flat, bias, and dark images that were taken nightly. Reduction to the magnitude system was then performed automatically by the OurSolarSiblings (OSS) data pipeline (Fitzgerald 2018). This pipeline performs many functions, but the ones that were immediately relevant to this paper were as follows: the pipeline performed photometric calculations on the images through six different methods. These were the Source Extractor Aperture (SEX) and Source Extractor Kron (SEK) (Bertin and Arnouts 1996), Aperture Photometry Tool (APT) (Laher *et al.* 2012a, 2012b), Dominion Astrophysical Observatory Photometry (DAO) (Stetson 1987), DoPHOT (DOP) (Schechter *et al.* 1993; Alonso-García *et al.* 2012), and PSFEX (PSX) (Bertin 2011). The results of these methods were then organized into photometry catalogue files comparing the R.A. and Dec. with the x-y pixel location and the number of counts detected at that location and its error.

The next step was to search the image for potential comparison stars using various catalogues. These catalogues were: APASS DR1 for the B and V filters (Henden *et al.* 2009, 2016), Skymapper 1.1 for the *ip* filter (Wolf *et al.* 2018), and Pan-STARRS DR1 for the *zs* filter (Magnier *et al.* 2020; Flewelling *et al.* 2020). Calibration stars were chosen by the ASTROSOURCE package (Fitzgerald *et al.* 2021). ASTROSOURCE is a tool designed to interpret the output of the OSS pipeline. It first determines comparison stars of a sufficient signal-to-noise ratio across the whole data set for a specific filter. It then analyzes these potential stars to determine which have the least variable magnitudes across the data set. Using the stars with known magnitudes, listed in Table 3, ASTROSOURCE calibrates the stars that fulfil the above criteria to determine their magnitudes. These are then used to produce a differential magnitude light curve for the observed variable star, RU Cet.

The full list of calibration stars and their locations is given in Table 3. For this paper the light curve produced by the SEK method was chosen because it produced the light curve with the lowest amount of scatter to the eye. The SEK method has been used by many using the LCO telescopes to research RR Lyrae stars through the OurSolarSiblings RR Lyrae research course (Fitzgerald 2021). The SEK method can determine the apparent

Table 3. List of calibrator stars and calibrated magnitudes from the surveys listed in the text.

Calibration Star	R.A. (degrees)	Dec. (degrees)	Filters	B Magnitude	V Magnitude	<i>ip</i> Magnitude	<i>zs</i> Magnitude
CS1	15.1034613	-16.134187	B	12.465 ± 0.02	—	—	—
CS2	15.3044044	-15.861488	B, V, <i>ip</i> , <i>zs</i>	14.268 ± 0.03	13.631 ± 0.01	13.276 ± 0.006	12.2732 ± 0.0065
CS3	15.267423	-15.9739347	B, V, <i>ip</i>	13.518 ± 0.018	12.97 ± 0.019	12.681 ± 0.09	—
CS4	15.2740296	-15.8059527	B, V, <i>ip</i>	14.322 ± 0.02	13.459 ± 0.019	12.874 ± 0.004	—
CS5	15.2180487	-16.1363677	B, V, <i>ip</i>	14.241 ± 0.027	13.612 ± 0.034	13.295 ± 0.003	—
CS6	15.2773297	-15.8654621	<i>ip</i> , <i>zs</i>	—	—	13.243 ± 0.003	13.0735 ± 0.009
CS7	15.3122939	-15.8950456	<i>ip</i>	—	—	14.181 ± 0.005	—
CS8	15.2069684	-16.0582662	V	—	13.471 ± 0.009	—	—

Note: R.A. and Dec. are provided in ICRS degree format. CS1 is also identified as TYC 5848-2346-1.

Table 4. Results derived in this work.

Measurement	Units	Filter			
		B	V	ip	zs
Average magnitude	Magnitude	$12.006 \pm 0.002$	$11.690 \pm 0.001$	$11.535 \pm 0.002$	$11.583 \pm 0.002$
Pstring	Days	$0.588 \pm 0.016$	$0.586 \pm 0.025$	$0.588 \pm 0.023$	$0.584 \pm 0.0295$
PPDM	Days	$0.586 \pm 0.015$	$0.585 \pm 0.019$	$0.584 \pm 0.014$	$0.584 \pm 0.019$
Magnitude range	Magnitude	1.413208	1.05476277	0.8153254	0.70325996

Note: Average magnitude is the error-weighted average apparent magnitude. Magnitude range is the difference between the data minimum and maximum magnitudes. P stands for period. String refers to the string length minimization method and PDM refers to the phase dispersion method.

magnitude of stars and galaxies with consistency (Bertin and Arnouts 1996). Accurately determining the magnitude of our observed star and comparison stars is important to determining the distance to our star, and will be elaborated further in section 3. In total, the following numbers of measurements of magnitude were recovered in the SEK method from the images: 33 in the B filter, 34 in the V filter, 35 in the ip filter, and 32 in the zs filter.

### 3. Results

In this section we first discuss the derivation of the period, average apparent magnitude, and metallicity of RU Cet. These quantities are then applied to compute the distance to the star. We consider first the derivation of the period.

Period finding and light curves were produced by ASTROSOURCE. Two methods of period finding are implemented, being the string length minimization method (Dworetzky 1983) and the phase dispersion method (Stellingwerf 1978). These are both standard methods, having the advantage that they are model-independent. No assumption is made of the form of the underlying function, only that there is a repeating signal, in this case a period. Altunin *et al.* (2020) developed a method to automate these processes across data sets, and this method is incorporated into the ASTROSOURCE program. We report the period averaged from eight derived periods. We present folded light curves (Figures 2–5) only for periods derived from the PDM method for each filter.

We next address the question of whether the light curve is adequately sampled to derive a convincing distance estimate. Our light curves are not sampled as densely as we would have wished, due in part to the steep rise of RU Cet. Notably, a single datum defines the brightest magnitude. The data set is complete enough for our purpose, as demonstrated in the next three paragraphs where we compare our periods and magnitudes with those from other studies.

The period of RU Cet was determined through averaging the eight period values presented in Table 4. This was an unweighted average. The result,  $0.585 \pm 0.020$  day, is in good agreement with those of other authors. Two examples: from the All Sky Automated Survey (ASAS) Szczygiel *et al.* (2009) derive a period of 0.5862844 d, and from the Catalina Sky Survey (CSS) Drake *et al.* (2013) derive a period of 0.5862768 d.

The average apparent magnitude, from which our distances are determined, was determined for each filter as an error-weighted average of measured magnitudes,  $m_j$ ,

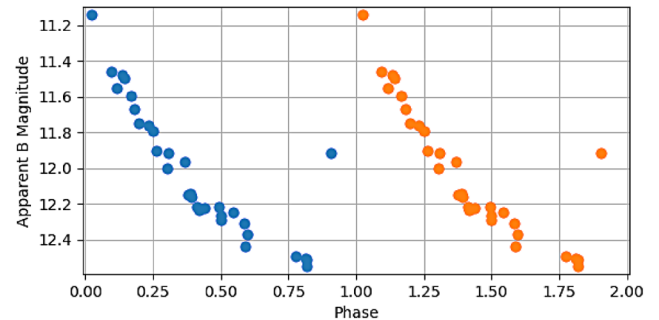


Figure 2. Folded lightcurve in the B filter with the PDM method applied.

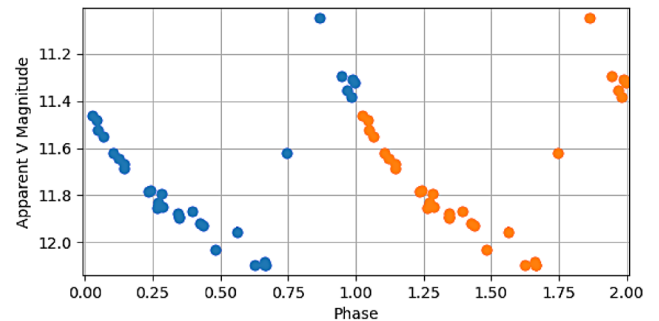


Figure 3. Folded lightcurve in the V filter with the PDM method applied.

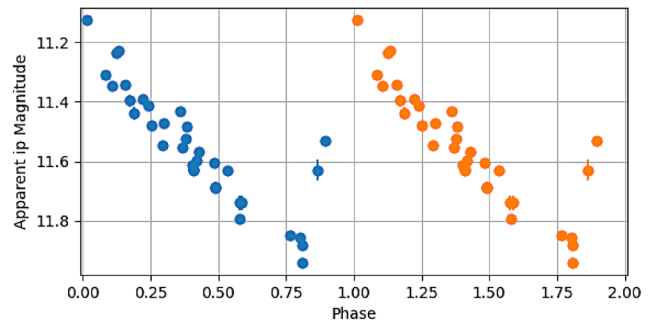


Figure 4. Folded lightcurve in the ip filter with the PDM method applied.

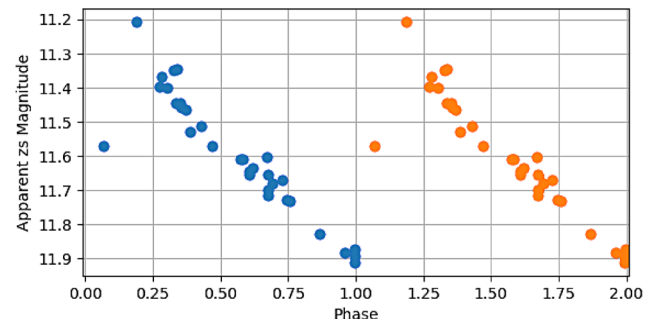


Figure 5. Folded lightcurve in the zs filter with the PDM method applied.



$$\text{Average magnitude} = \frac{\sum m_j / \sigma_j^2}{\sum 1 / \sigma_j^2} \quad (1)$$

In the V-band, we observed a magnitude range of 11.045–12.099, an average magnitude of  $11.690 \pm 0.001$ , and an amplitude of 0.527. As a check on our weighted average we also computed an average magnitude by integrating the phased light curves. We used the trapezoid rule. The trapezoid averages were statistically indistinguishable from the weighted averages. Our average magnitude values correspond well with those of other authors. For example, citing again the ASAS analysis, Szczygiel *et al.* (2009) list a magnitude range of 11.101–12.034, an average magnitude of 11.689, and an amplitude of 0.465 mag. Our average V-magnitude is statistically identical to that of ASAS. We use the average apparent magnitude to determine a photometric distance.

RU Cet exhibits variations in both magnitude range and period. Variations in period are best-studied. The Groupe Europeen d'Observations Stellaires (GEOS) RR Lyrae database (Le Borgne *et al.* 2007) maintains a list of times of maxima of a large group of RR Lyrae field stars, including RU Cet. The most recent ephemeris for this star was published by Vandebroere *et al.* (2014). They reported a period derived from observations of 97 maxima between 1890 and 2012, being 0.58628706 with a standard deviation of 0.1787 day. The brightest points recorded on our light curves were collected near JD 2459153.87; the GEOS database records a maximum near JD 2459153.84. Our observation is about 40 minutes after maximum, or about 5% of the period. The true brightest magnitude could be a tenth of a magnitude brighter than our observed value in V, a few hundredths of a magnitude in the infrared filters. This error then would be the largest error in our analysis.

We consider here the question of metallicity. Measured [Fe/H] values are summarized in Table 1. We adopted a value for [Fe/H] of  $-1.5 \pm 0.2$ , a midpoint between the lowest and highest values from the literature. This quantity is converted to a metals/hydrogen ratio [M/H] via (Salaris *et al.* 1993):

$$[M/H] = [\text{Fe}/\text{H}] + \log(0.638 \times 10^{0.3} + 0.362) \quad (2)$$

We then applied a conversion to  $\log(Z)$  via (Catelan *et al.* (2004) and Cáceres and Catelan (2008)):

$$\log Z = [M/H] - 1.765 \quad (3)$$

Absolute magnitudes for RU Cet were obtained using the following relations (the  $M_V$ -metallicity relation comes from Catelan *et al.* (2004), while the  $M_I$ - and  $M_Z$ -metallicity relations come from Cáceres and Catelan (2008)):

$$M_V = 2.288 + 0.882 \log Z + 0.108 (\log Z)^2 \quad (4)$$

$$M_I = 0.908 - 1.035 \log P + 0.220 \log Z \quad (5)$$

$$M_Z = 0.839 - 1.295 \log P + 0.211 \log Z \quad (6)$$

In these equations,  $M$  is the absolute magnitude of the source star,  $P$  is the period (days), and  $Z$  is the metallicity.

Solving for the absolute magnitudes allows us to compare them to the apparent magnitudes, derived from the observations using the photometry methods described in section 2. The equation used to compare the two is:

$$d = 10^{\frac{m-M-A+5}{5}} \quad (7)$$

Here,  $m$  is the average apparent magnitude, derived through the photometric methods described in section 2. The large  $M$  is absolute magnitude, derived through the theoretical equations listed above. The  $A$  is the value for interstellar extinction. We solved for distance,  $d$ , and extinction,  $A$ , simultaneously thus: we chose the value of color excess,  $E(B-V)$ , that minimized the standard deviation computed from three distance values  $d_V$ ,  $d_{ip}$ , and  $d_{zs}$ , i.e., the distance derived in each of the V, ip, and zs filters using extinctions  $A_V$ ,  $A_{ip}$ , and  $A_{zs}$ . We used the standard relations for extinction, e.g.,

$$R_V = \frac{A_V}{E(B-V)} \quad (8)$$

with  $R_V = 3.1$ . We derived a color excess of  $E(B-V) = 0.004$  mag. An estimate of the maximum extinction along the line of sight to RU Cet is provided by Schlafly and Finkbeiner (2011) via online query of the NASA/IPAC Infrared Science Archive. Their value is  $E(B-V) = 0.0207$  mag, a bit larger than our value. Given the patchiness of extinction and the high galactic coordinates of RU Cet ( $b = 78^\circ$ ,  $l = 134^\circ$ ) the extinction is plausibly very small.

Calculating a weighted average of the distances in the different filters given above, we obtain an average distance of  $1636 \pm 33$  parsecs to RU Cet. The Gaia Early Data Release 3 (EDR3) distance value for RU Cet is  $1699 +83 / -75$  parsecs (median of the photogeometric distance; Bailer-Jones *et al.* (2021)). The differences between the calculated values here and the Gaia EDR3 value are of order 1 to 2 standard deviations.

#### 4. Conclusion

This research used observations of the RR Lyrae star RU Cet to test the infrared period-luminosity-metallicity (PLZ) relationships put forward by Catelan *et al.* (2004) and Cáceres and Catelan (2008). The period was determined to be  $0.585 \pm 0.020$  days. The distance to RU Cet was determined to be  $1633 \pm 33$  pc. The difference between the PLZ value and the Gaia EDR3 value is 66 parsecs, which is between 1 and 2 times the uncertainties. The PLZ method thus yields consistent results. This consistency is reassuring given the changing period of RU Cet.

Suggestions for future work would include inventing and testing further refinements to the PLZ relations, continued regular monitoring of RU Cet for changes in period and magnitude range, and a better estimate of the interstellar extinction.

#### 5. Acknowledgements

Thank you to Michael Fitzgerald for his help in setting up the OurSolarSiblings RR Lyrae research course, as well

as the work put into developing an efficient data pipeline and software to make the research process incredibly easy to apply and understand.

We also thank the referee for many helpful suggestions upon the manuscript.

This research has made use of the SIMBAD database, operated at CDS, Strasbourg, France.

This research has made use of the International Variable Star Index (VSX) database, operated at AAVSO, Cambridge, Massachusetts, USA.

This work has made use of data from the European Space Agency (ESA) mission Gaia (<https://www.cosmos.esa.int/gaia>), processed by the Gaia Data Processing and Analysis Consortium (DPAC, <https://www.cosmos.esa.int/web/gaia/dpac/consortium>). Funding for the DPAC has been provided by national institutions, in particular the institutions participating in the Gaia Multilateral Agreement.

The DSS image is based on photographic data obtained using The UK Schmidt Telescope. The UK Schmidt Telescope was operated by the Royal Observatory Edinburgh, with funding from the UK Science and Engineering Research Council, until 1988 June, and thereafter by the Anglo-Australian Observatory. Original plate material is copyright© the Royal Observatory Edinburgh and the Anglo-Australian Observatory. The plates were processed into the present compressed digital form with their permission. The Digitized Sky Survey was produced at the Space Telescope Science Institute under US Government grant NAG W-2166.

This research has made use of SAOImageDS9, developed by Smithsonian Astrophysical Observatory.

This research has made use of the NASA/IPAC Infrared Science Archive, which is funded by the National Aeronautics and Space Administration and operated by the California Institute of Technology.

## References

- Alonso-García, J., Mateo, M., Sen, B., Banerjee, M., Catelan, M., Minniti, D., and von Braun, K. 2012, *Astron. J.*, **143**, 70 (DOI: 10.1088/0004-6256/143/3/70).
- Altunin, I., Caputo, R., and Tock, K. 2020, *Astron. Theory Obs. Methods*, **1** (DOI: 10.32374/atom.2020.1.1).
- Bailer-Jones, C. A. L., Rybizki, J., Foesneau, M., Demleitner, M., and Andrae, R. 2021, *Astron. J.*, **161**, 147 (DOI: 10.3847/1538-3881/abd806).
- Bertin, E. 2011, in *Astronomical Data Analysis Software and Systems XX*, eds. I. N. Evans, A. Accomazzi, D. J. Mink, A. H. Rots, ASP Conf. Ser. 442, Astronomical Society of the Pacific, San Francisco, 435.
- Bertin, E., and Arnouts, S. 1996, *Astron. Astrophys., Suppl. Ser.*, **117**, 393 (DOI: 10.1051/aas:1996164).
- Bessell, M. S. 1993, in *Stellar photometry - Current techniques and Future Developments*, eds. C. J. Butler, I. Elliott, IAU Colloq. 136, Cambridge Univ. Press, Cambridge, 22.
- Brown, T. M., et al. 2013, *Publ. Astron. Soc. Pacific*, **125**, 1031 (DOI: 10.1086/673168).
- Cáceres, C., and Catelan, M. 2008, *Astrophys. J., Suppl. Ser.*, **179**, 242 (DOI: 10.1086/591231).
- Catelan, M., Pritzl, Barton J., and Smith, H. A. 2004, *Astrophys. J., Suppl. Ser.*, **154**, 633 (DOI: 10.1086/422916).
- Chiba, M., and Yoshii, Y. 1998, *Astron. J.*, **115**, 168 (DOI: 10.1086/300177).
- Cusano, F., et al. 2021, *Mon. Not. Roy. Astron. Soc.*, **504**, 1 (DOI: 10.1093/mnras/stab901).
- Drake, A. J., et al. 2013, *Astrophys. J.*, **763**, 32 (DOI: 10.1088/0004-637X/763/1/32).
- Dworetzky, M. M. 1983, *Mon. Not. Roy. Astron. Soc.*, **203**, 917 (DOI: 10.1093/mnras/203.4.917).
- Feast, M. W., Laney, C. D., Kinman, T. D., van Leeuwen, F., and Whitelock, P. A. 2008, *Mon. Not. Roy. Astron. Soc.*, **386**, 2115 (DOI: 10.1111/j.1365-2966.2008.13181.x).
- Fitzgerald, M. 2018, *Robotic Telesc. Student Res. Education Proc.*, **1**, 343 (DOI: 10.32374/rtsre.2017.033).
- Fitzgerald, M. 2021, private communication.
- Fitzgerald, M., Gomez, E., Salimpour, S., Singleton, J., and Wibowo, R. 2021, *J. Open Source Software*, **6** (DOI: 10.21105/joss.02641).
- Flewelling, H. A., et al. 2020, *Astrophys. J., Suppl. Ser.*, **251**, 7 (DOI: 10.3847/1538-4365/abb82d).
- Fukugita, M., Ichikawa, T., Gunn, J. E., Doi, M., Shimasaku, K., and Schneider, D. P. 1996, *Astron. J.*, **111**, 1748 (DOI: 10.1086/117915).
- Graham, J. A., and Slettebak, A. 1973, *Astron. J.*, **78**, 295 (DOI: 10.1086/111416).
- Henden, A. A., Templeton, M., Terrell, D., Smith, T. C., Levine, S., and Welch, D. 2016, *VizieR Online Data Catalog: AAVSO Photometric All Sky Survey (APASS) DR9, II/336*.
- Henden, A., Welch, D., Terrell, D., and Levine, S. 2009, *Bull. Amer. Astron. Soc.*, **41**, 669.
- Kolenberg, K., Guggenberger, E., and Medupe, T. 2008, *Commun. Asteroseismology*, **153**, 67 (DOI: 10.1553/cia.153s67).
- Kovács, G. 2005, *Astron. Astrophys.*, **438**, 227 (DOI: 10.1051/0004-6361:20052742).
- Laher, R. R., Gorjian, V., Rebull, L. M., Masci, F. J., Fowler, J. W., Helou, G., Kulkarni, S. R., and Law, N. M. 2012a, *Publ. Astron. Soc. Pacific*, **124**, 737 (DOI: 10.1086/666883).
- Laher, R. R., et al. 2012b, *Publ. Astron. Soc. Pacific*, **124**, 764 (DOI: 10.1086/666507).
- Layden, A. C. 1994, *Astron. J.*, **108**, 1016 (DOI: 10.1086/117132).
- Layden, A. C., Hanson, R. B., Hawley, S. L., Klemola, A. R., and Hanley, C. J. 1996, *Astron. J.*, **112**, 2110 (DOI: 10.1086/118167).
- Le Borgne, J. F., et al. 2007, *Astron. Astrophys.*, **476**, 307, 283 (DOI: 10.1051/0004-6361:20077957).
- Magnier, E. A., et al. 2020, *Astrophys. J., Suppl. Ser.*, **251**, 3 (DOI: 10.3847/1538-4365/abb829).
- Neeley, J. R., et al. 2019, *Mon. Not. Roy. Astron. Soc.*, **490**, 4254 (DOI: 10.1093/mnras/stz2814).
- Preston, G. W., Shectman, S. A., and Beers, T. C. 1991, *Astrophys. J.*, **375**, 121 (DOI: 10.1086/170175).
- Salaris, M., Chieffi, A., and Straniero, O. 1993, *Astrophys. J.*, **414**, 580 (DOI: 10.1086/173105).
- Sandage, A. 1993, *Astron. J.*, **106**, 687 (DOI: 10.1086/116675).

- Schechter, P. L., Mateo, M., and Saha, A. 1993, *Publ. Astron. Soc. Pacific*, **105**, 1342 (DOI: 10.1086/133316).
- Schlafly, E. F., and Finkbeiner, D. P. 2011, *Astrophys. J.*, **299** 737, 103 (DOI: 10.1088/0004-637X/737/2/103).
- Stellingwerf, R. F. 1978, *Astrophys. J.*, **224**, 953 (DOI: 10.1086/156444).
- Stetson, P. B. 1987, *Publ. Astron. Soc. Pacific*, **99**, 191 (DOI: 10.1086/131977).
- Szczygiel, D. M., Pojmański, G., and Pilecki, B. 2009, *Acta Astron.*, **59**, 137 (<https://arxiv.org/abs/0906.2199>).
- Tonry, J. L., *et al.* 2012, *Astrophys. J.*, **750**, 99 (DOI: 10.1088/0004-637X/750/2/99).
- Vandenbroere, J., Le Borgne, J.-F., and Boninsegna, R. 2014, *GEOS Circ. RR53* (July), 1 (<http://geos.upv.es/index.php/publications/func-startdown/1519/>).
- Watson, C. L., Henden, A. A., and Price, A. 2006, in *The Society for Astronomical Sciences 25th Annual Symposium on Telescope Science*, Society for Astronomical Sciences, Rancho Cucamonga, CA, 47.
- Wolf, C., *et al.* 2018, *Publ. Astron. Soc. Australia*, **35**, e010 (DOI: 10.1017/pasa.2018.5).